RSC Sustainability

ROYAL SOCIETY OF CHEMISTRY

PAPER

View Article Online
View Journal | View Issue

Cite this: *RSC Sustainability*, 2025, **3**, 2377

On decoating of polymer electrolyte-based solid-state battery cathodes†

Anna Thielen, *[a] Thomas Leißner,[a] Tobias Eisenmann[b] and Urs A. Peuker*[a]

Received 7th February 2025
Accepted 29th March 2025

DOI: 10.1039/d5su00082c

rsc.li/rscsus

It is assumed that solid-state batteries (SSBs) represent a significant advancement in battery technology, offering a range of benefits over traditional lithium-ion batteries (LIBs). Nevertheless, there has been a scarcity of research examining the sustainability of these materials, with only a limited number of recent studies focusing on recycling concepts. In this study we examined the process behaviour of polymer based composite cathodes. For this, we identified the most suitable comminution principles to separate the cathode active material (CAM), polymeric solid-state electrolyte (SSE) and conductive additives from the electrode foil. In addition to thermal pre-treatment of the cathodes with subsequent dry mechanical stressing in a hammer mill, stressing in a wet agitated media mill was found to be a particularly suitable processing approach. Based on these findings, a preliminary process design for recycling polymer-based SSBs is proposed.

Sustainability spotlight

The timely development of a recycling process before waste is generated is extremely important in achieving the goal of reducing waste. This study presents processes for recycling polymer-based solid-state battery cathodes, providing an opportunity to reintroduce these materials into the lifecycle of solid-state batteries. The decoating process plays a central role in the recovery of active materials. By using a wet agitated media mill with distilled water as the liquid, a decoating efficiency of 98% was achieved, allowing the potential recovery of all components through subsequent mechanical and chemical processes. This represents an advantage over thermal treatment and the associated loss of organic materials. Our work therefore highlights the importance of the UN sustainable development goal of responsible consumption and production (SDG 12) and encourages the pursuit of affordable and clean energy (SDG 7) and industry, innovation, and infrastructure (SDG 9).

1. Introduction

Currently, lithium-ion batteries (LIBs) dominate the global battery market due to their use in electric mobility applications. The market share of LIBs has experienced robust annual growth, ranging from 30% to over 40% in recent times. However, the scope for further optimization of liquid electrolyte-based LIBs is diminishing, and the technology is anticipated to reach its limits in the next decade.[1] Therefore, it is essential to investigate alternative or next-generation technologies. One promising option is solid-state batteries (SSBs). These types of batteries offer the potential for significantly increased energy density and improved safety by eliminating flammable liquid electrolytes and thus preventing electrolyte leakage and explosion risks associated with liquid organic electrolytes using solid-state electrolytes (SSEs).[2–4] Additionally, SSEs are expected to hinder the growth of lithium dendrites due to their high mechanical rigidity, which facilitates the use of lithium-metal anodes allowing for increased energy density.[2,5,6] The ongoing development of SSBs presents an opportunity to strategically devise and execute recycling processes for sustainability, given that these batteries are not yet widely produced.[7] However, the recycling of SSBs remains largely unexplored.[7–9] Despite their substantial market potential, research on recycling processes for SSBs to reclaim critical raw metals for a circular economy is limited.[3] The importance of battery recycling technologies should not be overlooked when researching new battery concepts and materials, as demonstrated by the example of conventional LIBs. The ecological and economic considerations have made the recycling of LIBs increasingly important.[10–12] In recent years, there has been growing interest in recycling opportunities due to the increasing demand for critical metals, environmental concerns related to the mining of raw materials, improper disposal of spent LIBs, and legal requirements.[11,13–15] For example, the new regulation 2023/1542 of the European Parliament and of the Council of 12 July 2023 on batteries and waste batteries stipulates a certain percentage of recycled content in batteries, targets for recycling efficiency and targets for recovery of materials.[15]

[a]*Institute of Mechanical Process Engineering and Mineral Processing, Technische Universität Bergakademie Freiberg, Agricolastraße 1, D-09599 Freiberg, Germany. E-mail: anna.thielen@mvtat.tu-freiberg.de; urs.peuker@mvtat.tu-freiberg.de; Tel: +49 3731 39 3665*

[b]*BMW AG, D-80788 Munich, Germany*

† Electronic supplementary information (ESI) available. See DOI: https://doi.org/10.1039/d5su00082c

2. Recycling of LIBs (state of the art)

The recycling process of lithium-ion batteries (Fig. 1) usually begins with deactivating or discharging the battery system.[7,16,17] The level of discharge has an impact on the properties and material composition of functional units, which in turn affects the characteristics of recycling products.[18] The deactivation is followed by dismantling down to cell modules or individual cells. Afterwards, three main process technologies – mechanical, hydrometallurgical, and pyrometallurgical – are used, often in combination, to break down battery components into material streams with specifications suitable for synthesizing new materials.[7,16,17] Mechanical processing is often referred to as a pre-treatment process and is particularly crucial for hydrometallurgical technologies and direct recycling of spent LIBs. It plays a vital role in enhancing recovery efficiency and reducing energy consumption in subsequent recycling processes.[19,20]

The discharging and dismantling of lithium-ion batteries is typically followed by shredding, resulting in fragments of casing, electrodes, separators, and a powder fraction known as black mass, which is a mixture of decoated cathode and anode active materials.[21] Typical methods used for comminution include shear crushing and impact milling. The latter is primarily used to separate the electrode material from the current collector foil rather than for the initial opening of the cells.[22] The more intensive the stress becomes, the better the decoating efficiency and the black mass yield of recovery are.[22–26] However, the level of contamination from the electrode foil in the black mass product also increases,[24,25] which negatively affects its quality and the market price. After comminution, classification and various separation techniques are used to separate the fragments for further recycling.[17,24,25] Mechanical separation techniques are based on different physical properties such as particle size, density, conductivity, and magnetic properties.[7,17,27] Mechanical processes are carried out sequentially, with multi-stage shredding and screening proving highly effective in improving the separation of coating and foil, resulting in increased yield and reduced contamination in each fraction.[17,24] The dry mechanical method described here can result in black mass yields of up to 96%, depending on both the battery type processed and the machines and operating parameters used.[22–26] Alternatively, mechanisms such as dissolving the binder in a suitable solvent or decomposing the binder at high temperatures can be used as process steps to separate the current collector foil from the particulate coating.[20,24] Black mass yields up to 99% are reported on the lab scale if the binder is dissolved, depending on the process parameters. Typically, *N*-methyl-2-pyrrolidone (NMP) is used as a solvent since polyvinylidene fluoride (PVDF) is used as a binder for cathodes.[24,28,29] Thermal pre-treatment (calcination or pyrolysis) can enable a black mass yield up to 99% depending on the temperature (500–600 °C) and treatment duration.[26,30–33] From 2032 on these processes will have to fulfil material-specific recovery rates of up to 95% due to legislation at least within the EU.[15]

In general, the main objective of mechanical pre-treatment is to produce a product as pure as possible, while at the same time achieving a high recovery of valuable materials.[13,17,25] While all

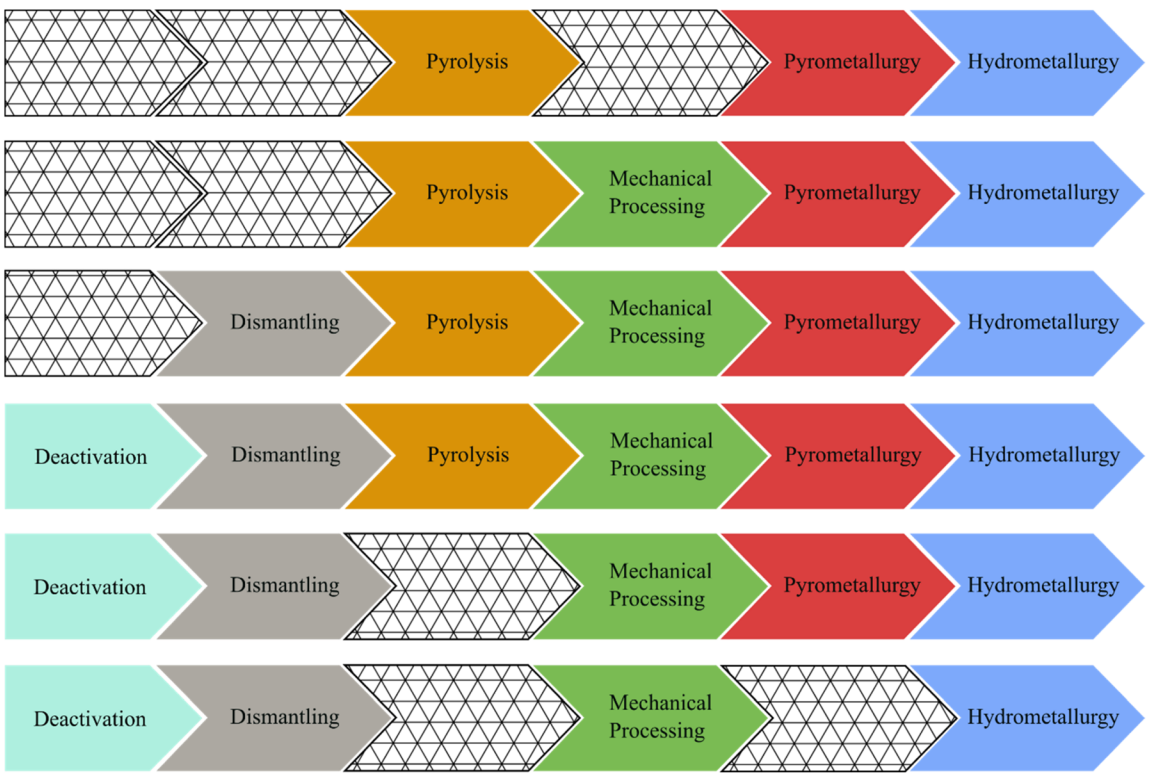

Fig. 1 An overview of potential recycling process chains in different combinations.

components of the cell, such as the anode, cathode, separator and electrolyte, contribute significantly to the cost of the cell, the cathode, which contains valuable materials such as cobalt and nickel, is the most expensive component, accounting for approximately half of the material cost.[1] As a result, most processes are specifically designed to maximize the recovery of the black mass.[13,17,22,25] Furthermore, the earlier mentioned high material-specific recovery rates required by regulation 2023/1542 of the European Parliament and of the Council of 12 July 2023 on batteries and waste batteries[15] serve to reinforce this position. The black mass can be further separated and processed using hydrometallurgy or direct recycling techniques.[7,12,25] It should be noted that the product characteristics achieved by the mechanical processes, such as the level of impurities, will affect the subsequent metallurgical processes and the quality of the recovered metals.[34,35]

More in-depth reviews on processes in the field of recycling of lithium-ion batteries are described by Doose *et al.*[16] and other experts.[13,14,19,34,36]

3. Approaches for the recycling of SSBs (specifically polymer electrolyte-based)

Research on SSBs has been conducted on various electrolyte chemistries and manufacturing methods, which has led to progress towards commercialization. At present, solid-state electrolyte (SSE) materials with the highest potential can be categorized into four groups: halide electrolytes, oxide electrolytes, sulfide electrolytes, and polymer electrolytes.[1] Lithium metal is a popular choice for the anode due to its high specific capacity and low redox potential.[2,16] However, there has been insufficient study on the sustainability of these materials, as there have only been limited recent studies focusing on recycling concepts.[7,9,37]

The integration of lithium-metal anodes and solid electrolyte chemistries in SSBs presents novel challenges to the recycling processes currently employed for LIBs, which are about to be implemented on pilot and production scales.[7,9,16] Therefore, these processes may not be directly applicable to SSBs and may require adjustments for effective recycling in the future.[9,17,38,39] However, it is uncertain whether these adjustments can achieve recycling rates similar to those of established recycling processes for conventional LIBs. These processes enable at the moment rates exceeding 90% for individual materials, depending on process combinations.[16,17]

Another challenge arises from the limited sample quantity available for research into recycling methods due to the parallel development of SSB systems and the corresponding efficient recycling processes. A reduction in the test scale compared to research with conventional LIBs may therefore be necessary under certain circumstances. In addition to technical aspects, it is important to consider which materials have to be recycled preferentially based on legal requirements and economic value.[38]

Polymer electrolytes are the most established of all solid electrolytes in terms of material availability and production technologies.[1] Their main advantages over inorganic solid electrolytes include cost, ease of processing and material flexibility.[1] However, challenges remain such as limited ionic conductivities at room temperature, poor chemical compatibility with high potential cathode active materials and low limiting current density due to the ionic conduction mechanism.[1,4,40] Polymer electrolytes based on polyethylene oxide (PEO) present a low risk, although the hygroscopic nature of PEO makes it susceptible to water absorption.[7,8]

In mechanical processes such as shredding and screening, the flexibility of polymer SSEs can be a challenge, especially when separating black mass from current collectors or passing through sieves.[7,8] However, an additional washing step using a suitable solvent such as water or water/alcohol mixtures can facilitate the separation of PEO-based polymeric SSEs and current collector foil.[7,8,16] Undissolved solids can be removed by filtration and other separation methods. Ideally, the resulting solution would contain PEO monomers and lithium salts, which can be converted back to SSEs by heating and solvent removal.[7,8] However, it remains uncertain whether this can be achieved with sufficient quality or purity, as even small amounts of dissolved polymer electrolytes significantly alter the solution viscosity and affect the precipitation of metal ions.[7,8,16] Another option for separating polymeric SSE is pyrolysis or pyrometallurgical treatment, in which the SSE is burned off. While this method allows the exposed materials to be further processed similar to traditional LIBs, it results in the loss of the polymer SSE.[8,16]

However, all these approaches are mainly theoretical considerations. Their practical applicability has yet to be tested.

4. Materials, methods, and calculations

The materials and methods utilized in the experiments are described in detail in the following sections. This includes a comprehensive overview of the equipment, chemicals, and other resources employed during the experimental process and the procedures followed to conduct each experiment. Furthermore, the analytical methods applied to interpret the data are explained, along with the specific calculations used to derive the results.

4.1. Materials

The objective of this study was to examine the process behaviour of polymer cathodes in the context of potential adaptations to existing recycling processes for conventional LIBs. Therefore, in addition to polymer electrolyte-based SSB cathodes, conventional LFP cathodes were also investigated in certain experiments. The cell type, from which the conventional LFP cathode was manually extracted, was a cylindrical cell with a mass of around 197 g and a capacity of 4 A h. More detailed information about the cell type can be found in Wilke *et al.*[41] The aluminium current collector foil of this cathode is coated

on both sides. The total mass of the cathode is made up of approximately 26% aluminium.

The surface of the aluminium current collector foil of the polymer electrolyte-based SSB cathodes is protected with a carbon primer. Compared to the conventional and commercial LFP cathodes used in the recycling experiments, the current collector in this case is only coated on one side. The coating is a homogeneous mixture of lithium iron phosphate (LFP), polyethylene oxide (PEO), conductive salt (LiTFSI) and carbon black. LFP represents the largest proportion of the coating mass, accounting for 72 wt%. Carbon black makes up 3.7% by weight of the coating mass. A more detailed description of the cathode can be found in the work of Helmers *et al.*[42] The mass of the aluminium current collector foil was determined experimentally by decoating individual cathode pieces by soaking them in a water bath for 24 hours. The coating and primer could then be completely removed by gently brushing the surface. The current collector accounts for 11 ± 1% of the total mass of the cathode.

4.2. Methods

For the decoating experiments (Fig. 2), both types of cathodes were manually cut into 5 mm × 5 mm squares. Samples of a weight of 336 ± 25 mg were prepared. The polymer cathode samples were stored at 21 °C and a relative humidity of 18% until they were processed. All experiments were carried out thrice.

First, the decoating behaviour of conventional commercial LFP cathodes and polymer cathodes under dry mechanical stress was investigated. The experiments were carried out with a hammer mill (picocrush, Hosokawa Alpine AG; Augsburg, Germany). In order to minimize metallic contamination from the current collector foil in the fine fraction, the largest sieve mesh size (1 mm × 2 mm) was selected for the hammer mill. A total of nine different rotational speeds were tested (3000 rpm/5000 rpm/7000 rpm/10 000 rpm/12 000 rpm/15 000 rpm/20 000 rpm/25 000 rpm/30 000 rpm). The duration of each batch test was always 30 seconds. After the comminution the sample was then sieved (0.315 mm/0.6 mm/1 mm/2 mm) to create a particle size distribution (PSD). Subsequently, the size classes with $x >$ 315 μm were sorted manually to determine the mass of the residual coated current collector and the free coating. The black mass product ($x <$ 315 μm) was analysed using inductively coupled plasma optical emission spectroscopy (ICP-OES) (iCAP 6300, Thermo Fisher Scientific Inc.; Waltham, United States) to determine the percentage of aluminium impurities.

In light of the insights obtained from the recycling of conventional LIBs, the decoating behaviour of polymer cathodes that had undergone thermal treatment was also examined. Both cryogenic comminution and mechanical stressing of samples after calcination were tested. Based on thermogravimetric analyses carried out in-house, a temperature of 350 °C was set for calcination. A treatment duration of 90 minutes was selected, which has also been used in the literature.[43] The mechanical stressing of the samples was carried out with the hammer mill under the conditions described earlier. Further processing of the samples and their analysis were also carried out as described earlier (sieving, manual sorting, ICP-OES). Cryogenic comminution was performed using a ball mill (CryoMill, Retsch GmbH; Haan, Germany) with a grinding chamber volume of 50 ml. A single 25 mm diameter ball was used as the grinding media. The sample was first pre-cooled using liquid nitrogen for 10 min at a frequency of 5 Hz. The sample was then stressed six times for 1.5 min at 15 Hz. After each stress interval an intermediate cooling of 1 min at 5 Hz was performed.

Two different machines/experimental set-ups were tested as part of the wet mechanical decoating process. In the first lab-scale set-up, the samples were agitated in a beaker containing 300 ml of distilled water for varying periods of time (45 min/90 min/180 min/360 min) using a magnetic stirrer. After the respective time had elapsed, the current collector pieces were removed from the water with tweezers. The pieces were then dried and weighed. The coating particles remaining in the water were analysed regarding their particle size distribution using laser diffraction (HELOS/KF, Sympatec GmbH; Clausthal-Zellerfeld, Germany). A second wet decoating option was

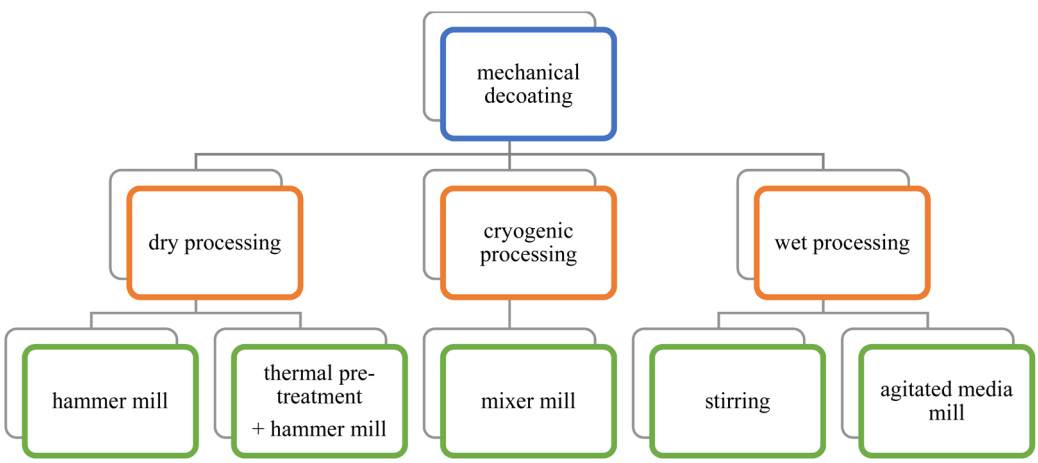

Fig. 2 Experiments (green) carried out on the different approaches (orange) for mechanical decoating.

evaluated by testing the use of a wet agitated media mill (picoliq, Hosokawa Alpine AG; Augsburg, Germany). The volume of the process chamber was 25 ml, with a grinding media filling level of 80 vol%. The grinding balls had a diameter of 1 mm. The objective was to apply a minimal frictional load on the surface of the current collectors, thereby exerting an adjusted shear on the coating, to accelerate mechanically the decoating process while avoiding any damage to the current collectors. Consequently, the lowest possible speed of 1000 rpm was selected. The experiment duration was set at 5 and 10 minutes. The grinding balls and current collector pieces were then separated from the suspension by wet sieving. The pieces were again dried and weighed. The coating particles remaining in the water were analysed by laser diffraction, as was done in the stirring experiments.

The shape and surface of individual particles were analysed more closely using scanning electron microscope ESEM-FEG (XL 30, FEI; Waltham, United States). Images were obtained of the samples in SE (topography contrast) and BSE (material contrast) modes and the chemical composition was determined by means of energy dispersive X-ray analysis (EDAX – AMATEK, Genesis software).

4.3. Calculations

The mass-specific decoating efficiency (E_D) is defined as the proportion of coating that has been removed from the current collector during the process. It was calculated using eqn (1). The total amount of aluminium current collector foil present in the feed ($m_{ACCF,F}$) is first subtracted from the aluminium current collector foil in the product ($m_{ACCF,P}$), which still has an undetermined amount of residual coating. This value is then divided by the total coating mass in the feed ($m_{C,F}$). Based on the previously mentioned determined aluminium current collector foil mass (approx. 11%), the mass of the coating in the feed accounts for 89% of the total feed mass. The division gives the proportion of coating that remains on the current collector after the process. To obtain the decoating efficiency, the remaining coating percentage is subtracted from eqn (1).

$$E_D = 1 - \frac{m_{ACCF,P} - m_{ACCF,F}}{m_{C,F}} \quad (1)$$

Eqn (2) was used to calculate the coating recovery (R_C) into the black mass product ($x < 315$ μm). For the calculation, the mass of the coating in the black mass product ($m_{C,BM}$) was divided by the mass of the coating in the feed ($m_{C,F}$). The mass fraction of the coating in the black mass product was determined using ICP-OES.

$$R_c = \frac{m_{c,BM}}{m_{c,F}} \quad (2)$$

The comminution ratio of the current collector (r_{90}) indicates the extent to which the particle size of the current collector has changed as a result of the process. It was calculated using eqn (3). The particle size of the current collector in the feed is divided by the particle size at which 90% of the current collector mass of the product is present. The larger the value, the smaller the particle size of the product compared to the feed. With a value of 1, it can be assumed that little to no comminution of the current collector has taken place.

$$r_{90} = \frac{x_F}{x_{90,P}} \quad (3)$$

The various key figures are presented as a function of the peripheral speed of the comminution tools (v_i) to facilitate the independent presentation of results, irrespective of the design-related parameters of the machine. The peripheral speed was calculated using eqn (4), where n_i represents the varying speeds and r denotes the radius of the circle spanned by the comminution tools. This circle has a diameter of 40 mm.

$$v_i = 2\pi \cdot n_i \cdot r \quad (4)$$

5. Results and discussion

5.1. Dry mechanical decoating

The mechanical stressing of electrodes has so far mainly been realised in research using small pilot or laboratory-scale machines. However, the investigations presented in this paper are conducted on a very small scale. This means that the process space or impact circle diameter is approx. 10 times smaller than that with laboratory-scale machines. The behaviour of conventional LFP cathodes under dry mechanical stress in the hammer mill was recorded to ensure that any behaviour deviating from the expectations based on the experience gained to date in LIB recycling can be attributed to the new material system and not to different aspects related to the experimental design. This serves as a control and comparative value for polymer-based cathodes. The degree of decoating as a function of the rotational speed or peripheral speed of the comminution tools is shown in Fig. 3a. In the case of conventional LFP cathodes, an initial increase in decoating is observed with accelerating the rotational speed. The higher intensity of the stress, which is achieved by increasing the peripheral speed of the hammers, initially results in enhanced decoating of the cathodes. However, at higher speeds, this increase plateaus considerably. Consequently, any further energy input yields only a limited benefit. A comparable phenomenon can be observed in the comminution ratio and, consequently, the intrinsic particle size distribution (Fig. 3b). One explanation for this is that the particles traverse the sieve before the 30 seconds of stressing time has elapsed, thereby preventing any further stressing of the particles. An optical examination of the particles reveals two notable forms. Firstly, there are rounded, compacted particles, the majority of which exhibit a coating-free surface. Secondly, there are flat pieces with a residual coating (Fig. 4a). The allocation of the respective areas, which can be seen in Fig. 4a, was determined using EDX measurements (Fig. S1†). Possible inclusions of coating in the rounded particles and residual coating on the flat pieces may account for the derivation to achieve a 100% decoating efficiency. Nevertheless, the polymer-

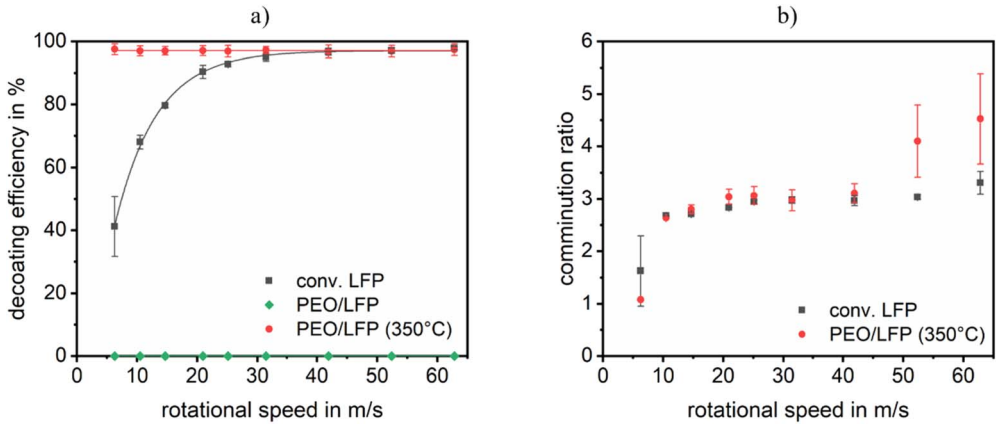

Fig. 3 Comminution results after mechanical stressing in a hammer mill at varying rotational speeds with (a) decoating efficiency and (b) comminution ratio of the current collector.

based cathodes display markedly different behaviour in the decoating efficiency, exhibiting no observable decoating. Thus, the PEO/LFP curve in Fig. 3a equals 0% decoating efficiency. Instead, only a deformation of the cathode pieces occurs. However, the bond between the coating and the current collector foil remains intact, as can be seen in Fig. 4b. Due to the adhesive properties of the coating, it was also not possible to perform a sieve analysis and thus a particle size analysis, as the individual particles adhered to each other. This leads to the conclusion that dry mechanical decoating by means of impact stressing (hammer mill) of untreated polymer-based cathodes is not possible.

Given that the polymer electrolyte, like the binders of conventional LIBs, is an organic material, the behaviour of thermally treated polymer-based cathodes was investigated as a further step. As can be seen in Fig. 3a, the 90-minute treatment

Fig. 4 Cathode sheet particles after mechanical stressing in the hammer mill at 25 m s^{-1} with (a) conventional LFP cathode, (b) PEO/LFP cathode, (c) PEO/LFP cathode with prior thermal treatment and (d) PEO/LFP cathode after cryogenic comminution.

of the cathodes at 350 °C demonstrates a notable decoating efficiency due to impact stressing for all milling parameters applied. Fig. 4c serves as an illustration. Nevertheless, in comparison to conventional LFP cathodes, more extensive exposure does not result in an increased decoating efficiency. The value is already considerably high at the lowest peripheral speed and remains largely constant at all other speeds. This phenomenon can be attributed to the extensive degradation of the bond between the coating and the current collector foil, which has been caused by the calcination of the organic components. Consequently, even minimal mechanical stress can result in the detachment of the residual coating. The comminution ratio of the polymer-based cathodes is comparable to that of conventional cathodes, as illustrated in Fig. 3b. However, at the two highest peripheral speeds tested, it appears that the current collector of the heat-treated polymer-based cathodes is reduced in size to a greater extent than that of the conventional cathodes. In conclusion, thermal pretreatment at elevated temperatures represents a potential strategy for decoating the current collectors by means of subsequent impact stressing.

The experiments conducted on cryogenic comminution did not yield the desired results with regard to decoating the current collector. In contrast to selective comminution, whereby solely the polymer-rich coating is subject to a reduction in particle size, both the coating and the current collector underwent a process of virtual pulverisation. However, the adhesive properties of the polymer caused the particles to agglomerate when the material was scraped out of the process chamber, resulting in the aluminium particles becoming embedded in the coating. This is illustrated in Fig. 4d. It can be concluded that the desired decoating could not be achieved using the earlier specified parameters. Nevertheless, it cannot be discounted that an alteration of the parameters may yield more favourable outcomes. However, in view of the unsatisfactory initial results, further investigation has not yet been undertaken.

Regarding subsequent hydro- or pyrometallurgical treatment processes, however, the recovery and contamination of the black mass product also represents a topic of interest. In the case of conventional LFP cathodes, it is evident that the recovery of the coating in the black mass product is proportional to the intensity (Fig. 5a). Given that the decoating of the current collector provides the foundation for the recovery of the coating, the resemblance in the two curves is to be expected. Nevertheless, the maximum recovery value is lower. This phenomenon can be attributed to several factors. As previously stated, the possibility exists that small quantities of coating may have become entrapped within the rounded particles, in addition to minor residual coatings on the current collector. Moreover, the overall mass loss observed during comminution increased from 2.50 ± 0.30% to 5.41 ± 3.18% for the conventional LFP cathodes. Furthermore, statistical deviations in the proportion of aluminium in the total mass of the cathode can also exert an influence on the calculated recovery value. It is also conceivable that not all coating agglomerates could be reduced to a particle size smaller than 315 μm because of mechanical stress and thus remain in the larger classes. However, it should be noted that while this is likely to have a significant impact on recovery at lower peripheral speeds, the proportion of coating agglomerates larger than 315 μm is unlikely to be considerable at the highest peripheral speeds. Nevertheless, this explains the different curves for the degree of decoating and coating recovery in the polymer-based cathodes. Although the stress intensity had no significant impact on the decoating process itself, due to the weakened bond between the current collector and the coating, the opposite is true regarding the recovery process. The formation of coating fragments is contingent upon the peripheral speed. At low speeds, larger fragments are produced, whereas at high speeds, the fragments are ground to a finer consistency. Compared to the conventional cathodes, however, it is noticeable that the recovery is even lower. This is due to the fact that, in addition to the previously mentioned reasons for the low maximum value for polymer-based cathodes, the loss of mass due to the calcination of the organic components of the coating is an additional complicating factor. This loss amounts to 25.65 ± 1.00% of the total cathode mass. Adding this mass loss to the recovery would give the yellow curve shown in Fig. 5a. This shows slightly better values at low circumferential speeds. At high speeds they are broadly in line with the recoveries

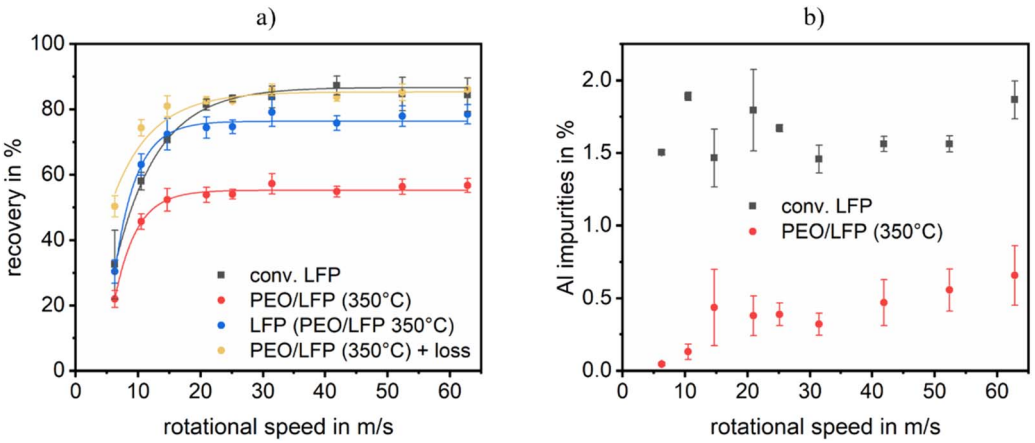

Fig. 5 Black mass product characteristics after mechanical stressing in the hammer mill at varying rotational speeds with (a) recovery and (b) Al impurities.

achieved with conventional LFP cathodes. This supports the assumption that the differences in recovery are largely due to thermal mass loss. The extent to which thermal pre-treatment affects coating recovery in conventional LFP cathodes or is comparable to the effect on polymer-based cathodes was not investigated in this experiment. If only the recovery of the LFP in the coating is considered, the values are more favourable. The visible difference in the recovery of conventional LFP cathodes can be attributed to the fact that the latter encompasses the entire coating, incorporating elements such as the binder and conductive salt.

The proportion of aluminium contamination of the black mass product (Fig. 5b) for the conventional LFP cathodes appears to fluctuate randomly around a value of 1.64 ± 0.16%. The slight increase in the comminution ratio (Fig. 3b) does not appear to have any effect here. One reason for this may be that the aluminium foil is more likely to be reduced in size, *i.e.* compacted, rather than shredded, and therefore accumulates in a particle size class with $x > 315$ µm. The aluminium contamination is still significantly higher than that observed for the polymer-based cathodes. As the conventional LPF cathodes were removed from used batteries, it is possible that the aluminium current collector was weakened due to ageing and degradation effects.[44] Compared to polymer-based cathodes, this could have led to an increased production of fine particles under mechanical stress. However, this assumption requires further verification. The observed differences could be influenced by manufacturing processes in addition to the effects of ageing/degradation. Aspects such as the binder amount,[45] coating thickness, and the calendaring process[46,47] are influencing factors of the adhesion strength.[48] While the adhesion strength should primarily affect the energy required for decoating, a stronger adhesion between the current collector and the coating, in combination with a weakened current collector due to factors such as aging has the potential to result in a higher degree of current collector contamination in the black mass product. However, given the absence of data regarding the age, usage, or manufacturing of the conventional LIBs employed in these experiments, no definitive conclusions can be drawn regarding the primary influencing factor on current collector contamination. As can be seen in Fig. 6, the mass of aluminium in the black mass is still greater in relation to the total mass of aluminium in the feed for the conventional LFP cathodes. The results for aluminium contamination of the black mass are therefore less due to the generally higher proportion of aluminium foil in the cathode mass. In contrast, the proportion of aluminium in the black mass product of polymer-based cathodes has been observed to increase with increasing circumferential speed and associated stress intensity. However, the values remain relatively low in comparison. Whilst thermal pre-treatment therefore enables dry decoating through impact stress (at low impurities), the low recovery rate motivates further solutions to be found.

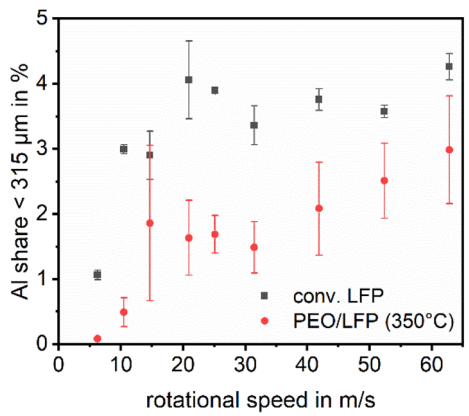

Fig. 6 Percentage of total aluminium (related to the cathode/feed) that has been found in the black mass product ($x < 315$ µm).

5.2. Wet mechanical decoating

The tests conducted on the solubility of PEO in water, as referenced in the literature with regard to the decoating behaviour of polymer cathodes in distilled water, yielded significantly more favourable results than the straightforward, dry, mechanical decoating process using the hammer mill. It is evident that the extent of decoating depends on the duration of agitation (Fig. 7a). Nevertheless, the increase between 180 min and 360 min is relatively modest. It is also noteworthy that the standard deviations for the 45- and 90-minute periods are relatively high. This observation can be attributed to the occasional collision and adhesion of cathodes on the coated side during the exposure time. This phenomenon hinders decoating, as sufficient contact with the water is not guaranteed. Consequently, the selected residence time is insufficient to loosen these bonds. It is also noteworthy that even after a treatment time of 360 minutes, complete decoating could not be achieved. As previously stated, this is attributable to statistical variations in the aluminium content of the cathode's total mass, which affects the calculated material yield. Additionally, minor coating residues were identified on the current collector foil (Fig. 7b). An analysis of the particle size distribution of the removed solid particles did not reveal any significant differences between the different exposure times (Fig. 8). This suggests that the stirring time has a minimal influence on the particle size of the removed coating particles. In comparison to the primary particle size of the LFP, which is approximately 0.49 µm, it can be assumed that the PSD measured here is composed of relatively big agglomerates. However, increasing the water temperature to 45 °C facilitates the dissolution of PEO in the water and can therefore significantly improve the decoating. In the case of stirring for 45 minutes it increases the decoating efficiency from 92.71% (at room temperature) to 96.05%, with a slight increase in variation. Even a shortened stirring time of only 10 min can achieve similar results to 45 min at room temperature. However, the previously mentioned problem of the cathode pieces sticking together causes problems here, which is reflected in a large fluctuation range.

However, with regard to industrial applications, a duration of 360 min may not be optimal, especially when a quite high dissolution of the PEO solution generated is required and therefore large quantities of water have to be used. In order to

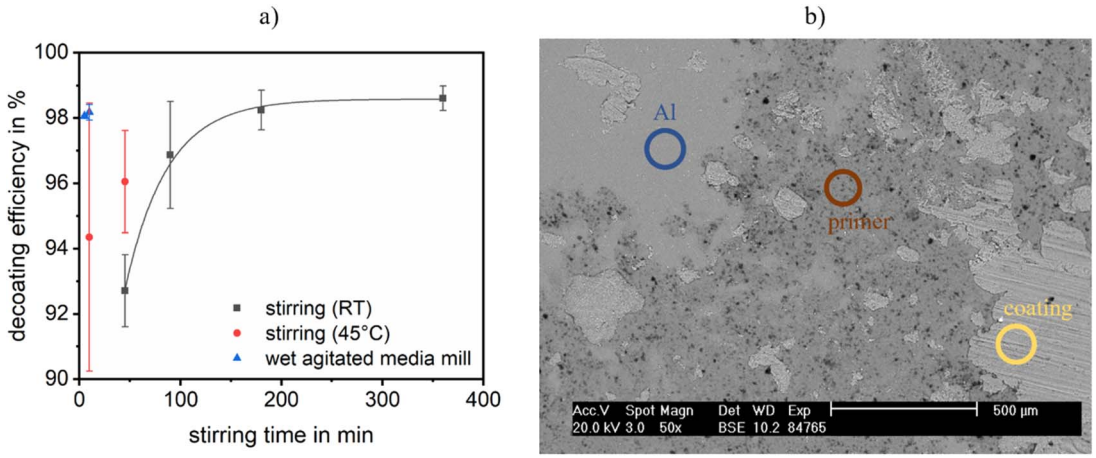

Fig. 7 Decoating results with (a) decoating efficiency at varying stressing times while using stirring (at room temperature and 45 °C) compared to the wet agitated media mill (b) surface of a cathode sheet particle that has been stirred for 360 min, where residues of the primer (red) and composite coating (yellow) can be seen on the aluminium foil (blue).

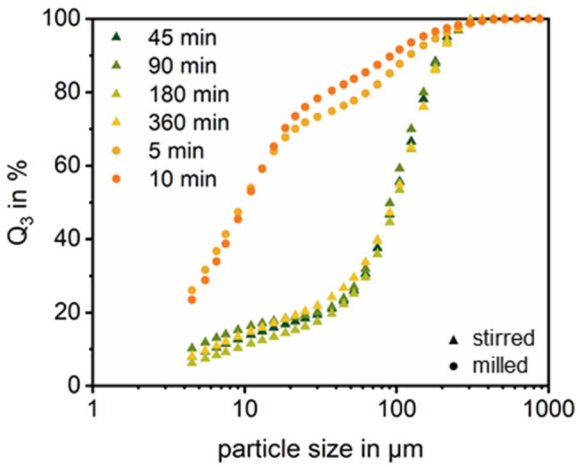

Fig. 8 Particle size distribution of wet decoating process products. The results with 5 min and 10 min are of tests in the wet agitated media mill. The remaining tests were carried out while stirring in a beaker.

accelerate the decoating process while avoiding any damage to the current collectors, a minimal friction load was applied to the surface of the current collectors using the wet agitated media mill. This process allows for a fast and significant reduction in coating, with a decoating efficiency of 98.18 ± 0.24% in a relatively short time frame of 10 min. A result comparable to that achieved after 180 minutes of simple stirring (RT) can be attained after a mere 5 min. The wet agitated media mill also performs better than the elevated temperature stirring experiments. However, whether the use of the mill is more energy efficient than stirring at elevated temperature needs to be investigated in future studies. In this case, an evaluation of the tests in terms of energy was not feasible or not particularly informative, given that the idle power of the mill was not exceeded.

Having a sharper lock on the particle size distribution (Fig. 8) it can be stated that both processes generate a LFP particle system between about 3 µm and 200 µm. However, the stirred media mill produced predominantly particles in the size range of below 20 µm showing only some larger clusters up to 200 µm. Thus, the milling not only decoats the aluminium foil but also breaks the coating, which affects the PEO between the particles. The gentle stirring does not disturb the PEO–matrix and the main effect of the liquid occurs at the aluminium–PEO-interface. Assuming a LFP primary particle size of 0.49 µm (according to Helmers *et al.*[42]) the overall picture shows that there are still aggregates of LPF-particles left for the milling treatment. These aggregates can originate from the original PEO matrix but also from depletion flocculation effects[49] in the PEO solution. For further processing and filtration to recover the PEO this effect has to be resolved. The efficiency and effectiveness of filtration and sedimentation are influenced by a range of factors. In this specific case, several challenges may arise. One of the primary factors is particle size. The decoating process can reduce the active material (LFP) to some extent down to its primary particle size, as shown in Fig. 8. Such fine particles tend to clog filter media, impeding flow and reducing filtration efficiency. This may necessitate pre-treatment steps such as flocculation to reduce filter loading and improve separation results. Another challenge lies in the viscosity of the solution. High concentrations of polyethylene oxide (PEO) can increase the viscosity of the solution.[50] Increased viscosity slows the flow of liquid through filters and hinders sedimentation by increasing the resistance to particle movement. Although recycling operations are typically performed near room temperature, slight heating—when compatible with the materials involved—can help reduce viscosity and thereby enhance both filtration and sedimentation rates. Further experimental investigations are therefore necessary in this case.

There are several potential recovery routes for recovering dissolved PEO from aqueous solutions. One possibility is precipitation by anti-solvent addition, where a non-solvent is added to the PEO-containing solution. This reduces the solubility of the PEO in water, leading to its precipitation.[51,52]

However, careful selection of the anti-solvent is required to ensure compatibility with other components present in the solution, and solvent recovery systems may be required to improve sustainability and reduce environmental impact. Another approach is temperature-induced precipitation, which exploits the lower critical solution temperature (LCST) behaviour of PEO in certain aqueous systems. When heated, PEO can undergo phase separation or precipitate out of solution.[51,53] The advantage of this method is that it avoids the need for additional chemicals and relies solely on thermal energy. However, it is important to note that the effectiveness of this method depends on factors such as the molecular weight of the PEO and its concentration in solution.[54] A third option is evaporation followed by recrystallization. In this process, the PEO solution is concentrated through evaporation, allowing PEO to crystallize as the solvent volume decreases. The disadvantage of this method is that it is energy intensive and there is a risk of thermal degradation of the polymer if high temperatures are used for long periods. Each of these recovery methods, and others not mentioned here, must be evaluated based on process conditions, desired purity levels, and sustainability considerations to determine the most appropriate approach for PEO recovery in the context of battery recycling.

5.3. Suggested recycling process

In light of the findings presented here regarding the decoating behaviour of polymer cathodes, it is recommended that the following process scheme be employed for the recycling of pouch cells with PEO as the solid electrolyte (Fig. 9). The initial stage of the process entails the shredding of the cells (for instance, using rotary shears or a granulator) in order to expose or open up the interior. Subsequently, the electrode foil is decoated in a wet state. It is recommended that a wet agitated media mill including a solvent suitable for the polymer be used, as this results in a significant reduction in the time required for this step compared to simple stirring due to the gentle frictional stressing of the surfaces. Following decoating, the product is subjected to wet classification to obtain the pouch cells and electrode foil. This foil mixture can then be further separated based on the existing mechanical processing technology for conventional LIBs (*e.g.* by aerostream classification). The remaining solid particles of the active material (LFP and conductive carbon black) are then separated from the solution by means of filtration/sedimentation.

The proposed recycling concept has so far only been tested for cathodes and requires further evaluation for pouch cells, where the presence of metallic lithium introduces additional challenges. When water comes into contact with metallic lithium in full pouch cells, several safety and efficiency concerns arise, posing significant obstacles to the recycling process. One of the primary safety risks is the highly exothermic reaction between lithium and water, which generates intense heat and can potentially lead to thermal runaway or even fire. Furthermore, the exothermic reaction produces hydrogen gas (H_2), which is highly flammable and can create an explosion hazard in confined spaces. Another critical issue is the formation of lithium hydroxide (LiOH), which can corrode battery components, compromising the integrity of materials and negatively affecting recyclability. Uncontrolled reactions may also introduce impurities into recovered materials, degrading the quality of the cathode and electrolyte components.

From an efficiency perspective, lithium–water reactions lead to the loss of valuable lithium, as lithium is converted into lithium hydroxide, making it more difficult to recover for reuse. Moreover, the necessity for additional process steps, such as neutralisation and gas handling, leads to an escalation in operational costs and complexity. The occurrence of side reactions has the potential to further degrade electrode materials,

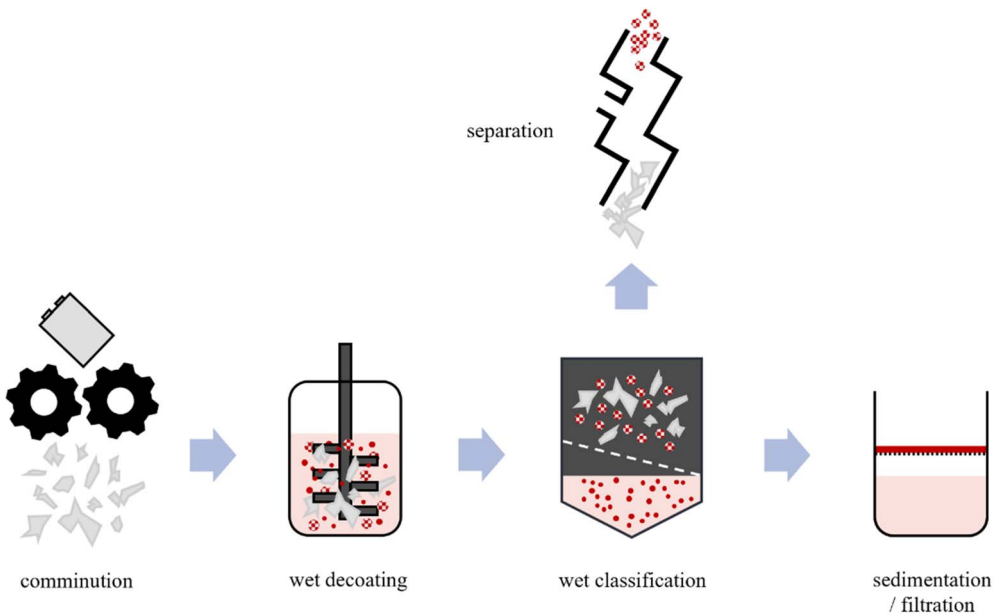

Fig. 9 Recommended process scheme for the recycling of pouch cells with PEO as the solid electrolyte.

thereby diminishing the yield of usable recovered materials and exerting an adverse effect on the overall economic feasibility of the recycling process.

In order to mitigate the aforementioned risks, it is imperative that several strategies are implemented. A key approach to this is controlled environment processing, which ensures that the first comminution step occurs in an inert atmosphere, such as argon or nitrogen, in order to prevent unintended lithium–water interactions. An alternative option would be to process in a dry carbon dioxide-rich environment (<4% oxygen), which would convert residual lithium metal to stable lithium carbonate compounds *via* reactions with CO_2.[7] In view of the fact that the formation of LiOH might be an unavoidable side process in this particular process, it is imperative that it is carried out under strictly controlled conditions. In order to minimize the severity of the reaction, water must be introduced at a regulated pH and temperature. Furthermore, effective gas management systems must be in place to ensure proper ventilation and hydrogen capture. This will prevent the accumulation of flammable gases and reduce the risk of explosions. This includes the consideration of a pressure equalisation valve when designing the wet agitated media mill.

6. Conclusion

The results presented here indicate that the direct transfer of the existing mechanical technology for processing conventional lithium-ion batteries (LIB) to solid-state batteries is not feasible. In the absence of prior thermal treatment of the cathodes, it was not possible to achieve dry mechanical decoating and thus the production of a black mass from a SSB cathode. However, a disadvantage of thermal pre-treatment is that approximately 25% of the total cathode mass is lost and therefore cannot be recovered. This can present a challenge in regard to recycling targets set out in laws and regulations. It is imperative to consider this aspect in light of forthcoming legal obligations. One potential solution is to subject the cathodes to stress in a wet medium. This approach allows for the decoating of the cathodes and the potential recovery of all components through subsequent mechanical and chemical processes. Based on these results, an initial concept for a possible recycling process was proposed. However, further testing is essential to ascertain the reliability of statements regarding the recovery of recyclable materials using this method. In addition, further research is required with a view to upscaling the experiments carried out here, optimising the operating parameters and an experimental verification of the process for pouch cells.

Data availability

The data supporting this article have been included as part of the ESI.†

Conflicts of interest

The authors declare no conflict of interest.

Acknowledgements

The research leading to these results received financial support from the BMW Group as part of the ALANO project (grant no. 03XP0396A) funded by the German Federal Ministry of Education and Research (BMBF). The authors would like to thank Dr Gert Schmidt of the Institute of Ceramics, Refractories and Composites for the SEM images in Fig. 4 and 7 and carrying out the respective EDX analyses. The authors would also like to thank Yvonne Volkmar for conducting the ICP-OES analysis and Annett Kästner for carrying out the laser diffraction measurements, as well as the remaining technical and scientific staff of the Institute of Mechanical Process Engineering and Mineral Processing. During the preparation of this work the authors used "DeepL Write" in order to improve the readability and language of the manuscript. After using this tool/service, the authors reviewed and edited the content as needed and take full responsibility for the content of the published article.

References

1 T. Schmaltz, *et al.*, *Solid-State Battery Roadmap 2035+*, Fraunhofer ISI, 2022.
2 J. Wu, *et al.*, Order-structured solid-state electrolytes, *SusMat*, 2022, **2**(6), 660–678.
3 K. Schneider, *et al.*, Acid Leaching of Al- and Ta-Substituted Li7La3Zr2O12 (LLZO) Solid Electrolyte, *Metals*, 2023, **13**(5), 834.
4 L. Wu, *et al.*, Interface science in polymer-based composite solid electrolytes in lithium metal batteries, *SusMat*, 2022, **2**(3), 264–292.
5 J. Janek and W. G. Zeier, A solid future for battery development, *Nat. Energy*, 2016, **1**(9), 16141.
6 A. Schreiber, *et al.*, Oxide ceramic electrolytes for all-solid-state lithium batteries – cost-cutting cell design and environmental impact, *Green Chem.*, 2023, **25**(1), 399–414.
7 L. Azhari, *et al.*, Recycling for All Solid-State Lithium-Ion Batteries, *Matter*, 2020, **3**(6), 1845–1861.
8 X. Wu, *et al.*, Toward Sustainable All Solid-State Li–Metal Batteries: Perspectives on Battery Technology and Recycling Processes, *Adv. Mater.*, 2023, 2301540.
9 L. Schwich, *et al.*, Recycling Strategies for Ceramic All-Solid-State Batteries—Part I: Study on Possible Treatments in Contrast to Li-Ion Battery Recycling, *Metals*, 2020, **10**(11), 1523.
10 X.-B. Cheng, *et al.*, A perspective on sustainable energy materials for lithium batteries, *SusMat*, 2021, **1**(1), 38–50.
11 S. Zhao, W. He, and G. Li, Recycling Technology and Principle of Spent Lithium-Ion Battery, in *Recycling of Spent Lithium-Ion Batteries: Processing Methods and Environmental Impacts*, ed. L. An, Springer International Publishing, Cham, 2019, pp. 1–26.
12 Y. Li, *et al.*, Recycling of spent lithium-ion batteries in view of green chemistry, *Green Chem.*, 2021, **23**(17), 6139–6171.
13 M. Chen, *et al.*, Recycling End-of-Life Electric Vehicle Lithium-Ion Batteries, *Joule*, 2019, **3**(11), 2622–2646.

14 Y. S. Zhang, *et al.*, A perspective of low carbon lithium-ion battery recycling technology, *Carbon Capture Sci. Technol.*, 2022, **5**, 100074.
15 EU, Regulation (EU) 2023/1542 of the European Parliament and of the Council of 12 July 2023 concerning batteries and waste batteries, amending Directive 2008/98/EC and Regulation (EU) 2019/1020 and repealing Directive 2006/66/EC, *Official Journal of the European Union*, 2023, **66**(L191), pp. 1–117.
16 S. Doose, *et al.*, Challenges in Ecofriendly Battery Recycling and Closed Material Cycles: A Perspective on Future Lithium Battery Generations, *Metals*, 2021, **11**(2), 291.
17 J. Neumann, *et al.*, Recycling of Lithium-Ion Batteries—Current State of the Art, Circular Economy, and Next Generation Recycling, *Adv. Energy Mater.*, 2022, **12**(17), 2102917.
18 A. Kaas, *et al.*, Influence of different discharge levels on the mechanical recycling efficiency of lithium-ion batteries, *Waste Manage.*, 2023, **172**, 1–10.
19 S. Kim, *et al.*, A comprehensive review on the pretreatment process in lithium-ion battery recycling, *J. Cleaner Prod.*, 2021, **294**, 126329.
20 J. Ordoñez, E. J. Gago and A. Girard, Processes and technologies for the recycling and recovery of spent lithium-ion batteries, *Renewable Sustainable Energy Rev.*, 2016, **60**, 195–205.
21 T. Lyon, *et al.*, Chapter 17 – Recycling battery casing materials, in *Nano Technology for Battery Recycling, Remanufacturing, and Reusing*, ed. S. Farhad, *et al.*, Elsevier, 2022, pp. 349–370.
22 Y. Ni, *et al.*, Effect of mechanical force on dissociation characteristics of cathode materials in spent lithium-ion batteries, *Process Saf. Environ. Prot.*, 2022, **161**, 374–383.
23 T. Lyon, T. Mütze and U. A. Peuker, Decoating of Electrode Foils from EOL Lithium-Ion Batteries by Electrohydraulic Fragmentation, *Metals*, 2022, **12**(2), 209.
24 C. Hanisch, *et al.*, In-Production Recycling of Active Materials from Lithium-Ion Battery Scraps, *ECS Trans.*, 2015, **64**(22), 131.
25 J. Diekmann, *et al.*, Ecological Recycling of Lithium-Ion Batteries from Electric Vehicles with Focus on Mechanical Processes, *J. Electrochem. Soc.*, 2017, **164**(1), A6184.
26 C. Hanisch, W. Haselrieder, and A. Kwade, Recovery of Active Materials from Spent Lithium-Ion Electrodes and Electrode Production Rejects. in *Glocalized Solutions for Sustainability in Manufacturing*, Springer Berlin Heidelberg, Berlin, Heidelberg, 2011.
27 X. Zhong, *et al.*, Pneumatic separation for crushed spent lithium-ion batteries, *Waste Manage.*, 2020, **118**, 331–340.
28 M. Ahuis, *et al.*, Direct recycling of lithium-ion battery production scrap -Solvent-based recovery and reuse of anode and cathode coating materials, *J. Power Sources*, 2023, **593**, 233995.
29 L.-P. He, *et al.*, Recovery of cathode materials and Al from spent lithium-ion batteries by ultrasonic cleaning, *Waste Manage.*, 2015, **46**, 523–528.
30 C. Hanisch, *et al.*, Recycling of lithium-ion batteries: a novel method to separate coating and foil of electrodes, *J. Cleaner Prod.*, 2015, **108**, 301–311.
31 W. Li, *et al.*, Study on Vacuum Pyrolysis Process of Cathode Sheets from Spent Lithium-Ion Batteries. in *REWAS 2019*, Springer International Publishing, Cham, 2019.
32 G. Lombardo, *et al.*, Comparison of the effects of incineration, vacuum pyrolysis and dynamic pyrolysis on the composition of NMC-lithium battery cathode-material production scraps and separation of the current collector, *Resour., Conserv. Recycl.*, 2021, **164**, 105142.
33 M. Mohr, *et al.*, Recycling of Lithium-Ion Batteries, *Encycl. Electrochem.*, 2020, 1–33.
34 S. Windisch-Kern, *et al.*, Recycling chains for lithium-ion batteries: A critical examination of current challenges, opportunities and process dependencies, *Waste Manage.*, 2022, **138**, 125–139.
35 O. A. Nasser and M. Petranikova, Review of Achieved Purities after Li-ion Batteries Hydrometallurgical Treatment and Impurities Effects on the Cathode Performance, *Batteries*, 2021, **7**(3), 60.
36 F. Larouche, *et al.*, Progress and Status of Hydrometallurgical and Direct Recycling of Li-Ion Batteries and Beyond, *Materials*, 2020, **13**(3), 801.
37 V. Kiyek, *et al.*, Waste minimization in all-solid-state battery production via re-lithiation of the garnet solid electrolyte LLZO, *J. Power Sources*, 2024, **609**, 234709.
38 N. Kononova, *et al.*, Identification of target materials for recycling of solid-state batteries from environmental and economic perspective using information theory entropy, *Proc. CIRP*, 2023, **116**, 185–190.
39 M. Fan, *et al.*, Progress in the sustainable recycling of spent lithium-ion batteries, *SusMat*, 2021, **1**(2), 241–254.
40 N. Boaretto, *et al.*, Lithium solid-state batteries: State-of-the-art and challenges for materials, interfaces and processing, *J. Power Sources*, 2021, **502**, 229919.
41 C. Wilke, A. Kaas and U. A. Peuker, Influence of the Cell Type on the Physical Processes of the Mechanical Recycling of Automotive Lithium-Ion Batteries, *Metals*, 2023, **13**(11), 1901.
42 L. Helmers, *et al.*, Sustainable Solvent-Free Production and Resulting Performance of Polymer Electrolyte-Based All-Solid-State Battery Electrodes, *Energy Technol.*, 2021, **9**(3), 2000923.
43 M. Ahuis, *et al.*, Recycling of solid-state batteries, *Nat. Energy*, 2024, **9**(4), 373–385.
44 A. Gabryelczyk, *et al.*, Corrosion of aluminium current collector in lithium-ion batteries: A review, *J. Energy Storage*, 2021, **43**, 103226.
45 B. Westphal, *et al.*, Influence of Convective Drying Parameters on Electrode Performance and Physical Electrode Properties, *ECS Trans.*, 2015, **64**(22), 57.
46 E. N. Primo, M. Touzin and A. A. Franco, Calendering of Li(Ni0.33Mn0.33Co0.33)O2-Based Cathodes: Analyzing the Link Between Process Parameters and Electrode Properties by Advanced Statistics, *Batteries Supercaps*, 2021, **4**(5), 834–844.

47 H. Zheng, *et al.*, Calendering effects on the physical and electrochemical properties of Li[Ni1/3Mn1/3Co1/3]O2 cathode, *J. Power Sources*, 2012, **208**, 52–57.
48 N. Billot, *et al.*, Investigation of the Adhesion Strength along the Electrode Manufacturing Process for Improved Lithium-Ion Anodes, *Energy Technol.*, 2020, **8**(2), 1801136.
49 M. Rudolph, *Nanoparticle-polymer-composites: the solution and spray drying process with an emphasis on colloidal interactions*, ed. A. Freiberger Forschungshefte, Techn. Univ. Bergakad, Freiberg, 2013.
50 M. I. Bahlouli, *et al.*, The Effect of Temperature on the Rheological Behavior of Polyethylene Oxide (Peo) Solutions, *Appl. Rheol.*, 2013, **23**(1), 13435.
51 B. Hanschmann, Precipitation of Polypropylene and Polyethylene Terephthalate Powders Using Green Solvents via Temperature and Antisolvent-Induced Phase Separation, *Adv. Polym. Technol.*, 2023, **2023**(1), 7651796.
52 J. G. Poulakis and C. D. Papaspyrides, Dissolution/reprecipitation: A model process for PET bottle recycling, *J. Appl. Polym. Sci.*, 2001, **81**(1), 91–95.
53 P. Pang and P. Englezos, Phase separation of polyethylene oxide (PEO)–water solution and its relationship to the flocculating capability of the PEO, *Fluid Phase Equilib.*, 2002, **194–197**, 1059–1066.
54 R. Hoogenboom, Chapter 2 – Temperature-Responsive Polymers: Properties, Synthesis, and Applications, in *Smart Polymers and Their Applications*, ed. M. R. Aguilar and J. San Román, Woodhead Publishing, Second Edition, 2019. pp. 13–44.